Temperature dependence of rotational disorder in a non-standard amino acid from X-ray crystallography and molecular dynamics simulation†

Birger Dittrich,*[a] John E. Warren,[b] Francesca P. A. Fabbiani,[c] Wolfgang Morgenroth[d] and Ben Corry[e]

Received 29th October 2008, Accepted 22nd January 2009
First published as an Advance Article on the web 20th February 2009
DOI: 10.1039/b819157c

The X-ray single-crystal structure of methyl 2-aminoisobutyrate hydrochloride (Me-AIB), a non-standard amino acid, is reported at 10, 30, 50, 70 and 100 K. Fourier maps indicate the presence of rotational disorder of the hydrogen atoms of the ester methyl group. To study this effect in detail, high resolution data were collected with synchrotron radiation. The non-spherical molecular electron density was predicted with invariom scattering factors and subtracted from the density obtained from a full multipole refinement. This allows disorder to be distinguished from the molecular electron density at each temperature. The disorder is reduced between 100 K and 30 K, but still detectable even at 10 K. Hence, difference densities can be applied for the purpose of electronic structure validation and have the advantage of an absence of noise over Fourier methods. Ultra-low temperature experiments are foreseen to be useful in reducing such kinds of disorder in ultra-high resolution protein crystallography. Molecular dynamics simulations of Me-AIB at temperatures between 10 and 100 K confirm the temperature dependence of the rotational motion of the methyl group seen experimentally. Modeling disorder in X-ray structure analysis will be an interesting future application of molecular dynamics simulations.

1. Introduction

In this paper we characterize rotational disorder using a difference-density approach. The compound studied, methyl 2-aminoisobutyrate hydrochloride, or methyl α-aminoisobutyrate hydrochloride (Me-AIB), is a derivative of α-aminoisobutyric acid (AIB), which is contained in some antibiotics of fungal origin, *e.g.* alamethicin and some lantibiotics. AIB is known to induce helices in peptides. Its crystal structure has been reported early[1] and has been recently redetermined.[2] Our interest in Me-AIB is fueled by the occurrence of rotational disorder in the methyl group attached to the alkoxy oxygen.

Tunneling of hydrogen atoms in methyl groups has been extensively studied by various techniques.[3] Acetic acid is a classical example where methyl rotation has been observed.[4,5] Aspirin and paracetamol[6–8] are two other examples that have been extensively studied by diffraction methods. The resolution-independent scattering length makes neutron diffraction a popular tool for studies of methyl rotation;[7,9] more recently the popularity of X-ray diffraction studies has increased.[10] By including the aspherical electron density in the scattering model[11] accuracy and precision of X-ray diffraction can be increased.

Disorder phenomena attract our interest for two main reasons. Firstly, disorder has been shown to be a major problem in successfully modeling the electronic structure of larger macromolecules of biological interest and weak scattering power.[12] Improving the available theoretical tools and likewise the experimental conditions in data acquisition is therefore imperative. Secondly, the interplay between static and dynamic processes is of high interest to understand drug–receptor interactions, and only when both are understood can we hope to gain deeper insight in these phenomena.‡ Compared to side chain disorder, where heavier nuclei are involved, rotational disorder of hydrogen atoms does not affect results from X-ray diffraction much. We focus on rotational disorder since it can be studied in full detail; our aim is to develop and improve methodology that can be also applied to dynamically disordered side chains of macromolecules at a later stage. Although a full understanding of the electronic structure is not usually required for routine structure analysis aiming to characterize molecular connectivity and conformation of small molecules (<200 atoms), disorder remains a major problem in both small molecule and macromolecular crystallography.

Temperature induced rotational disorder is not uncommon. However, it can be a small effect that goes unnoticed, and in the absence of high-resolution data it can slip past the attention of structure validation procedures. In small-molecule crystallography, disorder can usually be treated by partial occupancies.

[a] *Institut für Anorganische Chemie der Universität Göttingen, Tammannstr. 4, D-37077 Göttingen, Germany. E-mail: bdittri@gwdg.de*
[b] *SRS, Daresbury Laboratory, Daresbury, Warrington, UK WA4 4AD*
[c] *GZG der Universität Göttingen, Abt. Kristallographie, Goldschmidtstr. 1, D-37077, Germany*
[d] *Hasylab/DESY, Notkestr. 85, D-22607 Hamburg, Germany*
[e] *School of Biomedical, Biomolecular and Chemical Sciences, University of Western Australia, Crawley, WA, 6009, Australia*

† CCDC reference numbers 678215–678219. For crystallographic data in CIF or other electronic format see DOI: 10.1039/b819157c

‡ It should be noted that for understanding physiological processes an experiment temperature below the glass transition of proteins at 180 K conveys a certain artificiality.

However, this procedure is strictly only amenable when the data to parameter ratio is favorable. When larger molecules of biological interest are investigated, detailed modeling of disorder becomes infeasible as data resolution is usually severely limited. Yet it is for such cases that model improvements are needed most.

In this paper we initially characterize the rotational disorder by conventional Fourier methods, that give only a weak indication on the presence of disorder, but do not yield detailed information about its nature. To better characterize the disorder we extend methodology based on the invariom approach.[13] In the invariom method a theoretical electron density is represented by aspherical pseudoatoms[14] of the Hansen & Coppens[15] multipole model. The invariom database is a convenient way of generating accurate scattering factors to increase the information content obtainable from experimental single-crystal diffraction data within a structure factor formalism. Details of the procedure have been published elsewhere.[16] Other closely related database approaches[17,18] share this aim.

The invariom density can be directly compared to the result of a multipole refinement, since in both cases modeling is based on the same multipolar description. However, only the multipole refinement uses X-ray data to least-squares refine the multipole parameters that are flexible enough to also take into account disorder, whereas the invariom approach predicts those parameters from geometry optimized quantum chemical computations. Therefore thermal motion can be distinguished from the electron density by the difference of the theoretically predicted (invariom) and the 'measured' (multipole refinement) model electron density. For the title compound the difference allows to characterize rotational disorder in the ester methyl group.

Molecular dynamics simulations have long played a role in understanding the dynamics of both small molecules and large biological systems. Early simulations were crucial in forming our understanding of molecules as dynamic structures and careful simulations still provide one of the only ways to view the motion of individual atoms in time.[19] Molecular dynamics simulations have been conducted to study a number of topics relevant to X-ray crystallography; stability of crystal polymorphs[20] and crystal nucleation[21] are mentioned to name but a few, however, the use of such simulations for understanding crystal structure has been limited so far. In this study we use such simulations to better understand the disorder arising in crystal structures. These simulations allow us to view the nature and time scale of the rotational disorder by a method independent of the X-ray data, thus assisting our interpretation of the measured electron densities.

2. Experimental

Single crystals of the title compound were grown by slow evaporation of an aqueous solution. Diffraction data at 10 K

Table 1 Crystal and structure refinement data

Empirical formula	$C_5H_{12}NO_2Cl$				
Formula weight/g mol^{-1}	153.61				
Cell setting	Orthorhombic				
Space group, Z	*Pbca*, 8				
Temperature/°K	100	70	50	30	10
Unit cell dimensions:					
a/Å	8.6018(1)	8.5921(1)	8.5889(1)	8.5862(1)	8.553(2)
b/Å	8.7828(1)	8.7611(1)	8.7603(1)	8.7421(1)	8.713(3)
c/Å	22.2584(1)	22.2484(3)	22.2425(3)	22.2501(2)	22.141(2)
V/Å^2	1681.57(5)	1674.78(5)	1673.57(6)	1670.13(4)	1650.0(7)
Calculated density/g cm^{-3}	1.2135	1.2184	1.2193	1.2218	1.2367
F (000)	656.0				
Crystal size/mm	0.24 × 0.13 × 0.12				0.4 × 0.33 × 0.11
Crystal form, color	Rectangular, colorless				
Wavelength λ/Å	0.4750				0.5166
Absorption coefficient μ/[mm^{-1}]	0.125	0.126	0.126	0.126	0.164
Absorption correction	Empirical				none
Max. 2θ/°	63.88	63.69	63.85	66.50	50.98
(sin θ/λ)$_{max}$/Å^{-1}	1.11	1.11	1.11	1.11	0.83
No. of measured reflections	225652	220659	254489	260026	26274
No. of independent reflections	10582	10495	10540	10508	4257
No. of observed reflections	6161	7072	7556	7994	2977
Criterion for observed reflections	$F > 3\sigma(F)$				
Overall completeness	99.9%	99.1%	99.9%	99.9%	94.9%
Redundancy	21.2	20.4	24.0	22.2	4.3
Weighting scheme	Based on measured s.u.'s				
R_{int} (F^2) (%)	10.87	11.58	8.33	8.91	9.93
Number of parameters	82/83*				
N_{ref}/N_{var}	75.1	86.2	92.1	97.5	36.3
R_1 (F) (%)	3.54	3.29	2.70	2.02	3.50
R_w (F) (%)	4.02	3.44	2.82	2.28	4.22
R_{all} (F)† (%)	8.53	6.47	5.77	4.21	6.68
S†	2.25	2.08	2.16	1.66	1.41
$\Delta\rho_{max}$, $\Delta\rho_{min}$/e Å^{-3}	−0.55/0.77	−0.64/0.68	−0.75/0.69	−0.38/0.47	−0.72/0.35

$w = 1/\sigma^2$, $R_{int}(F^2) = \sum|F_o^2 - F_o^2\,(mean)|/\sum F_o^2$, *parameters additional to positions and anisotropic displacement parameters in the multipole refinement.

 This journal is © the Owner Societies 2009

were measured at the D3 beam line of the HASYLAB synchrotron in Hamburg using an Oxford Diffraction Helijet open flow helium cooling device. Reciprocal space was explored by a ϕ-scan at a distance of 43 mm and a wavelength of 0.5166 Å. The resolution of the 10 K synchrotron data was 0.83 in sin θ/λ and the XDS software[22] (version August 2006) was used for data reduction. An empirical correction for oblique incidence[23] of incoming high-energy X-rays on the detector material was applied.[24] High resolution data (sin $\theta/\lambda \geq 1.1$ Å^{-1}, $d < 0.45$ Å) at 30, 50, 70 and 100 K were measured at the station 9.8 of the SRS Daresbury[25] with an Oxford Cryosystems nHELIX open flow cooling device and a wavelength of 0.4750 Å. After data integration with SAINT (version 7.45A)[26] the correction for oblique incidence equally showed to be important due to the short wavelength and was performed with the version 2007/5 of the program SADABS.[27] The structure was solved with direct methods.[28] Further crystallographic data are listed in Table 1 and can be found in the CIF files of the ESI.‡

3. Methods

3.1. Structure factor modeling and least-squares refinements

Model structure factors were calculated using the Hansen and Coppens multipole formalism[15] as implemented in the program package XD.[29] In the invariom refinement modeling of the aspherical electron density was achieved by using individual invariom scattering factors, derived from eight model compounds *via* structure factors of simulated experiments.[30] The chloride atoms scattering was modeled by a conventional spherical Cl^- scattering factor. Bond distances to hydrogen atoms were set to values from the geometry optimized model compounds (DFT basis D95++(3df,3pd)) of the invariom database. Full details of the invariom modeling procedure were reported previously.[16] The respective model compounds for Me-AIB and their local atomic site symmetry can be found in Table 2.

We have also refined the electron density of the title molecule using a multipole model in which the predicted invariom parameters that are listed in Table 2 were freely refined, while the positions and the anisotropic displacement parameters (ADPs) were maintained. That way the number of parameters in the multipole refinement was reduced and it was ensured that molecular geometry for the calculation of the difference densities was identical. κ parameters were likewise kept fixed to the value of the invariom refinement. For hydrogen atoms only the bond directed monopole, dipole and quadrupole populations were refined, keeping the higher multipole populations fixed to the values of the invariom database.

The isotropic treatment of hydrogen-atom thermal motion has been shown to be inadequate for charge density studies.[31] A TLS-fit combining averaged internal modes from neutron diffraction allows the estimation of hydrogen atom ADPs and reduces the number of least-squares parameters.[32] We have included such estimated parameters for the H atoms in all refinements using the SHADE web server[33] for all temperatures. Input parameters for the rigid-body TLS fit (program THMA11)[34] of the ADPs of the heavy atoms involved were taken from the invariom refinements at the respective temperature.

Crystal quality and scattering power were somewhat limited, probably also due to the disorder present. Only highly intense synchrotron radiation allowed us to meet the resolution requirements of X-ray diffraction data in charge density modeling (sin $\theta/\lambda \approx 1.1$ Å^{-1}).[35]

3.2. Molecular dynamics

To investigate rotational disorder from a different perspective we undertook a molecular dynamics simulation for the crystal structure of Me-AIB using the NAMD package[36] and the CHARMM27 force field[37] at different temperatures in between 10 and 100 K in 10 K steps. Atomic charges were determined using the MK electrostatic fitting method from a HF/6-31+G(d) single point energy calculation with the program GAUSSIAN98[38] on the invariom geometry at 100 K. Molecular dynamics simulations were carried out on a 'super cell' containing 8 crystallographic unit cells ($2 \times 2 \times 2$) to allow standard cutoff lengths to be used for van der Waals interactions. Dynamics simulations were run under an NPT ensemble with a pressure of 1 atm during the simulations, each lasting 1 nanosecond using a time step of 1 fs. The Particle mesh Ewald method was used for computation of the electrostatic forces.[39,40] Long range electrostatic forces were evaluated every 100 fs. Periodic boundary conditions were imposed in all directions. For calculation of the time average of the distances between the atoms a tcl-script was written that aligned all molecules to an average one to remove rigid-body motion of the super cell.

Table 2 Details of invariom and multipole refinement for methyl 2-aminoisobutyrate hydrochloride

Atom	Invariom assigned	Site symmetry	Model compound	Chemically constraint to
Cl^-	Cl^-	—	Chloride ion	—
O1	O1c1c	*mm2*	Dimethylether	—
O2	O2	*m*	Formaldehyde	—
N1	N1c1h1h1h$^+$	*3*	Methylamide cation	—
C1	C2o1o1c	*m*	Acetic acid	—
C2	C1n1c1c1c	*3m*	Isoaminobutane	—
C3,4	C1c1h1h1h	*3*	Ethane	C3
C5	C1o1h1h1h	*3*	Methanol	—
H1A-C	H1n[1c1h1h]$^+$	*6*	Methylamide cation	H1A
H3&4A-C	H1c[1c1h1h]	*6*	Ethane	H3A
H5A-C	H1c[1o1h1h]	*6*	Methanol	H5A

4. Results and discussion

4.1. Visualizing rotational disorder

The atomic numbering scheme of the molecular structure of Me-AIB with atomic displacement parameters of the non-hydrogen atoms using the data measured at 10 K is shown in Fig. 1.

We initially applied Fourier methods to the 100 K diffraction data and observed features near the hydrogen atoms attached to C5 that indicate the presence of disorder. The plane of the three H atoms of the disordered C5 methyl group was chosen. Rather than completely omitting the H-atoms we included them in the model with a full occupancy, although this way the signal of the rotational disorder was weakened. Fourier residual maps of the independent atom model (IAM) in Fig. 2(a,c) and the invariom model, Fig. 2(b,d) are compared at two temperatures. Features are small and not well resolvable in the Fourier maps, as they are smeared due to thermal motion and the disorder present. However, all maps indicate that there is electron density missing in the middle of the circle formed by the three H-atoms and that additional density can be found along the vectors connecting two H-atoms. Replacing the spherical scattering factors of the elements by individual invariom ones, taking into account the bonding and lone pair density, removes noise from the maps. The signal does not get much stronger, though, since we have included the predicted anisotropic thermal motion of the hydrogen atoms in the invariom model as described above. Overall Fourier maps give a first indication that disorder is present, but we are not able to show that this is rotational disorder of the methyl group on this basis alone.

To improve the obtained signal we made use of recently introduced methodology.[42] By subtracting the invariom-model electron density from the density from a multipole refinement, disorder can be distinguished from molecular electron density. To obtain a clear signal, atomic positions should be identical

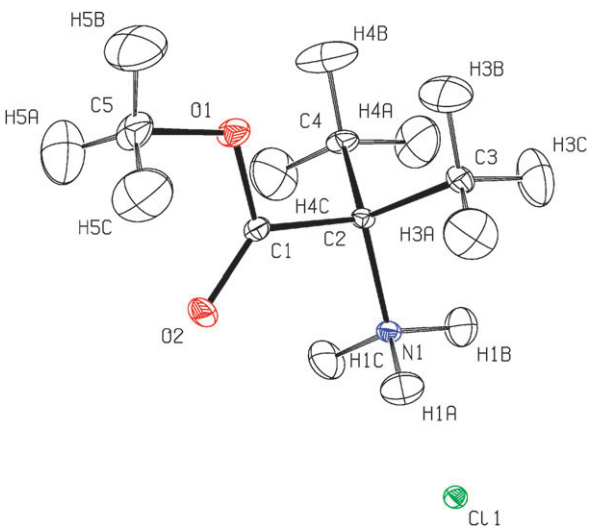

Fig. 1 ORTEP representation[41] of molecular structure and thermal motion at 10 K with atomic numbering schemes, thermal ellipsoids are shown at a probability of 50%. H-ADPs were obtained by combining external contributions from a rigid body fit with average values from neutron diffraction using the SHADE server.[33]

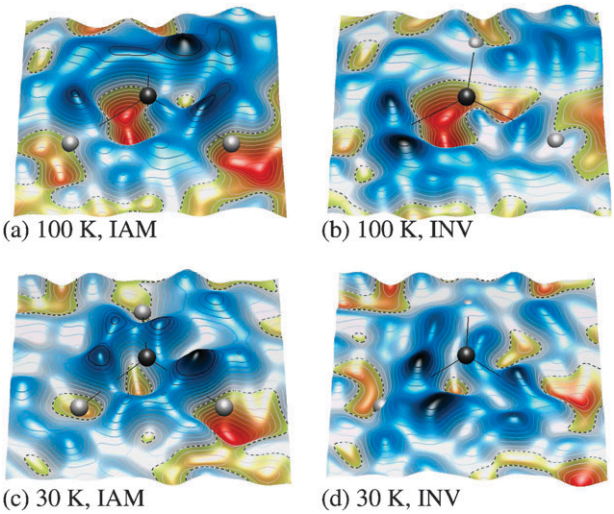

Fig. 2 Fourier residual maps of methyl 2-aminoisobutyrate hydrochloride in the plane of the H-atoms attached to C5. In (a) & (c) IAM means independent atom model, in (b) & (d) INV stands for invariom model; maps were calculated based on the refinements at 30 K and 100 K. A color gradient from red to blue was used to highlight negative to positive residual density. Each contour line represents an electron density of 0.025 e $Å^{-3}$, the zero contour is dotted.

and were fixed at the invariom result. The separation of electron density and dynamic motion is not unequivocal and relies on the fact that the multipole model can not distinguish between both effects. Refined multipole parameters can contain both electron density and disorder, whereas invariom model parameters reproduce a quantum mechanical electron density only. Hence, the difference density can only be as reliable as the database electron density is in predicting the molecular density, which has been shown to be in the order of 0.1 e $Å^3$.[42] Fig. 3 shows the differences between the invariom and multipole refinement at temperatures of 10 (a), 30 (b), 50 (c), 70 (d) and 100 K (e). At all temperatures significant differences of more than 0.2 e $Å^{-3}$ can be seen, which increase in intensity with temperature. As in our recent study on L-ornithine hydrochloride,[42] we would like to point out that the difference density is not a residual electron density (based on Fourier methods), as only modeled features of the two refinements are considered. We can therefore investigate small difference-density features un-blurred by effects of harmonic thermal motion with the two density models, which we will discuss in more detail below.

At 50, 70 and 100 K electron-density differences are visible in the proximity of the hydrogen atoms of the methoxy group. The density is not only different close to the moving hydrogen atoms, but also at O1 and O2, which will be discussed in detail later. The toroidal pattern that gains in intensity with increasing temperature at the H-atoms attached to C5 can obviously be explained by rotational disorder; when the H-atoms move away from the almost frozen position at 10 K their population is reduced, leading to red features in the difference maps (3). Further peaks in between the H-atoms start to emerge at 50 K, and form an almost toroidal shape of electron density at 100 K.

This journal is © the Owner Societies 2009

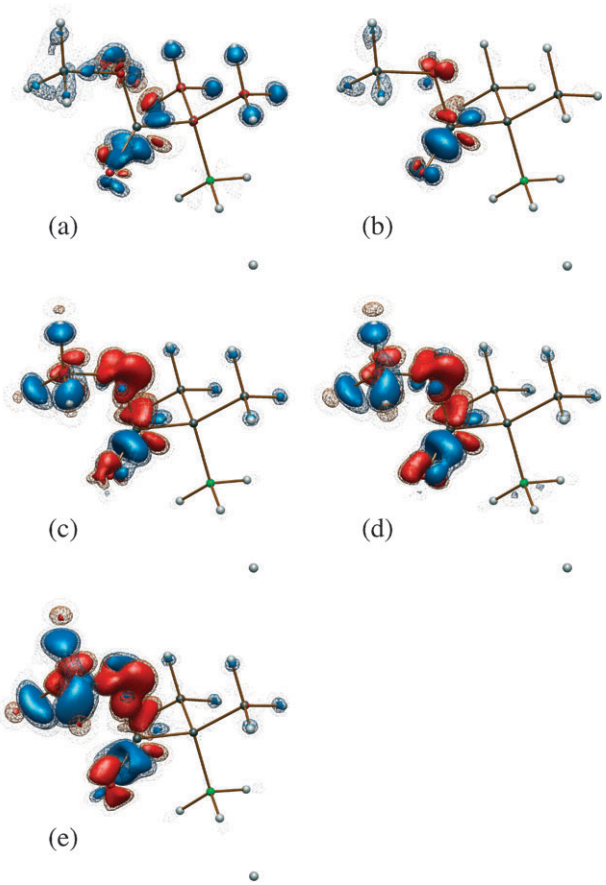

Fig. 3 Calculated difference between the electron density of the multipole minus the invariom refinements at 10 K (a), 30 K (b), 50 K (c), 70 K (d) and 100 K (e). This difference is not a residual density map, as only modeled features are considered. Iso-surfaces are 0.1 (dotted) 0.15 (meshed) and 0.2 e $Å^{-3}$ (filled). Positive features in blue, negative surfaces in red.

4.2. Temperature dependence of rotational disorder

Occurrence of such rotational disorder is common and some least-squares refinement programs[43] also allow it to be treated approximately in the scattering model. However, disagreements between experimental and model electron densities are usually not emphasized in routine structure reports. Going down in temperature the features mentioned are reduced to less than 0.1 e $Å^{-3}$ at a temperature of 30 K; even at 10 K they do not disappear completely, probably due to zero-point motion, or due to remaining conformational differences that are frozen out differently in different unit cells. We conclude that the disorder almost completely freezes out at very low temperatures in between 50 and 30 K and that such low temperatures are generally useful for determining structures to high accuracy. The reduction of the minimum and maximum residual density with temperature as listed in Table 1 supports this conclusion. Hence, the use of very low temperatures will also be beneficial for data collection and electron density studies of larger molecules of biological interest. Very low temperatures (a) improve the data to parameter ratio (see improvements between 100 to 30 K in Table 1) and (b) reduce atomic and molecular motion. However, the use of very low temperatures is not sufficient to solve practical modeling problems: The ensemble of atomic scattering factors and atomic displacement parameters is inadequate when atomic positions are smeared over a larger region in disordered structures. Conceptually the rotational motion of the methyl group forbids the assignment of the atomic scattering factor to just one defined position, as this can not completely reproduce the measured structure factors.

As stated above we have included an estimation of the ADPs of the hydrogen atoms. The inclusion of these estimates also for the H-atoms bound to C5 has an influence on the character and the strength of the signal—as has the sophistication of the multipole model (dipoles or quadrupoles). We have therefore included bond-directed quadrupoles in the refined multipole model. It is emphasized that the signal is strong enough to persist irrespective of the treatment of H-atom displacements or the sophistication of the multipole model, even when just monopoles are refined for the hydrogen atoms.

Density differences between an isolated molecule and one surrounded by other molecules in the crystal have been found to be small[44] and in the order of magnitude of 0.15 e $Å^{-3}$. As there were differences close to the oxygen atom of the carboxyl group between the measured and the theoretically predicted electron density exceeding influences that can be expected due to hydrogen bonding or the field of the surrounding molecules or ions, we tried to use a next-nearest neighbor model compound for the formally double-bonded oxygen atom O2. The scattering factor O2c was therefore altered to O2c[1o1c], and the model compound acetic acid replaced formaldehyde. We found that the *R*-factor was identical and the goodness of fit (GoF) even slightly worse when including next-nearest neighbors for O2. The Hirshfeld test[45] result, however, improved for both C—O bonds. Difference-density features near O2 were improved slightly, but not enough to justify general alteration of the well-established empirical rules for the choice of model compounds. We believe the invariom approach provides a good compromise between the accuracy and the number of model compounds required for electron density prediction of organic compounds, as indicated by the excellent agreement between predicted and measured electron densities in a recent study.[42]

4.3. Explaining the observed difference densities

Remaining electron density differences in Fig. 3, can be attributed to a number of factors. Apart from (i) possible differences in the local chemical environment in the whole molecule compared to the model compound just discussed, there may be (ii) shortcomings in the multipole model when de-convoluting electron density from thermal motion close to the oxygen nuclei. We have recently shown that differences in the predicted and measured electron density close to the oxygen atoms can be quite substantial (0.2 e $Å^{-3}$) using the example of the non-standard amino acid sarcosine.[44] The accuracy that can be achieved with the standard Hansen and Coppens (1978) multipole model can therefore be limited to 0.2 e $Å^{-3}$. However, in the case of Me-AIB such systematic modeling effects do not satisfactorily explain the observations, since the geometry and the thermal parameters in the experimental refinement were kept fixed at the invariom

geometry, thus systematic errors should cancel out. Further possible reasons for the relatively high difference in predicted and refined electron densities could be (iii) absorption effects or (iv) the lack of high-order reflections in the data sets. For all data measured at Daresbury, an empirical absorption correction has been applied, and at the short wavelength (high photon energy) we do not expect that absorption should have a major effect on the data, especially since differences occur only in one part of the molecule. Due to the limited number of parameters and the high data-to-parameter ratio in the experimental multipole refinement we are also confident about the significance of the populations parameters. (v) A further explanation might be that the underestimation of the population of the hydrogen atoms bonded to C5 is absorbed by the more electronegative O2 due to the overall charge constraint. However, this can also be ruled out, since the differences likewise occur for C1 of the ester group. To summarize we do not find explanations (i–v) convincing, as not only O2 but also C1 and O1 seem to be affected, whereas all other atoms only show rather small differences.

A more convincing explanation for the differences is that we actually see a concerted movement of the whole methoxy-ester group. It is well known and has been stated before that we can not observe electron density and thermal motion independent of each other,[46] and the basis of this study is to find ways to de-convolute these. As the lone pair electron density of both O1 and O2 will be interacting with the alternating density of the H-atoms we observe motion of the whole group together, the oxygen position responding to the rotational motion of the H-atoms. As a consequence C1 is also affected, being strongly covalently bonded to the oxygen atoms.

4.4. More insight from molecular dynamics simulations

This explanation is supported by the packing of the molecules in the crystal. Fig. 4 shows the crystal packing of Me-AIB. Neither O1 nor O2 are involved in classical hydrogen bonding. The structure is therefore separated into alternating layers in *c*-direction, one hydrogen bond involving the N–H···Cl interactions and another layer dominated by H-H contacts. Table 3 lists the three classical hydrogen bonds observed in the structure at 100 K. Non-classical C—H···O hydrogen bonds are supposedly even weaker than classical ones and possible acceptor atoms of O1 and O2 are further away than the threshold values usually applied.

We suggest that such an interaction-free environment is required and favorable to observe rotational disorder in general. Other crystal structures displaying similar features can probably easily be identified by investigating local packing environments around methyl groups with a similar flexibility to the ester-linkage in Me-AIB. We have measured the distances of the close contacts for the H5A-C atoms for the 100 K structure. Concerning the H-H contacts, the closest ones are between H4B and H5C with a distance of 2.26 Å and between H4B and H5A with 2.91 Å. The distance of H5C to the oxygen atom O1 is 2.84 Å and that of H5B to O2 is 3.01 Å. While the conformation adopted in the structure is likely to be the one with the lowest energy, closer contacts, whether attractive or repulsive, will occur during the rotation of the methyl group.

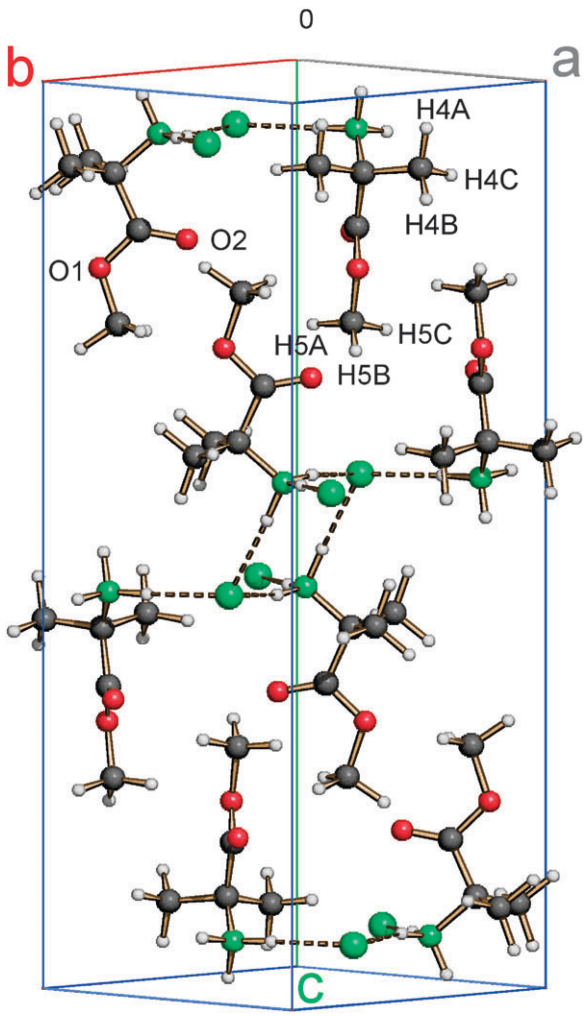

Fig. 4 Crystal packing (SCHAKAL representation[47]) of the Me-AIB. It can be seen that the methyl hydrogens attached to O1 have no near neighbors within 2.2 Å and are not restricted in their motion.

Our primary interest in the molecular dynamics simulations was whether it is possible to reproduce the temperature dependent rotational movement of the hydrogen atoms. We find that we can indeed see this in our simulations. This is shown in Fig. 5b, where we display the H5B–C5–O1–C1 torsional angle, which alternates between the three possible low-energy conformations at a temperature of 80 K. Interestingly the three H-atoms also occupy an intermediate position for some of the time, which is probably why we can observe rotational disorder in X-ray diffraction experiments. It is notable that neither of the other two methyl groups show this rotational disorder, in agreement with the X-ray data. A graphical representation of the disorder can be achieved by plotting the volume occupied by each of the hydrogen atoms as shown in Fig. 5a (generated with VMD[48]). VMD can provide probability distribution on a grid. This has interesting applications also for modeling other kinds of disorder involving heavier nuclei. A fundamentally new idea in this work is therefore, to obtain information and model thermal motion independent of electron density with molecular dynamics and use this information to improve the

 This journal is © the Owner Societies 2009

Table 3 Hydrogen bonding scheme for methyl 2-aminoisobutyrate hydrochloride

D–H···A	Symm. op.	D–H	H···A	D···A	D–H···A
N1–H1A···Cl1	x, y, z	1.02	2.15	3.1653(4)	172
N1–H1B···Cl1	$\frac{1}{2} + x, \frac{1}{2} - y, 1 - z$	1.02	2.17	3.1799(5)	169
N1–H1C···Cl1	$\frac{3}{2} - x, -\frac{1}{2} + y, z$	1.02	2.16	3.1563(4)	164

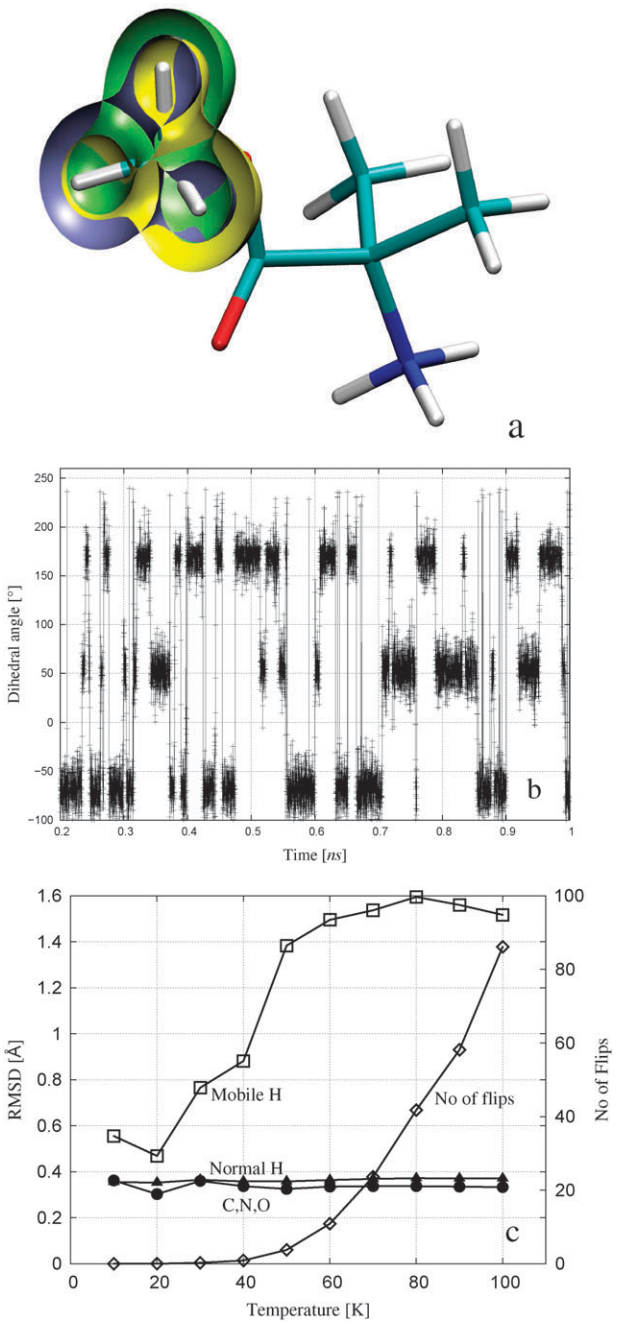

Fig. 5 (a) Probability distribution of the hydrogen atoms of the alkoxy group displayed with VMD.[48] (b) Dihedral angle between H5B–C5–O1–C1 at 80 K indicating rotational disorder. (c) Root mean square displacements of H atoms, the alkoxy H atoms and the non-H-atoms *versus* temperature. Only above 30 K the motion is observed in the simulation. The number of rotational 'flips' per *ns* of the C5 methyl group hydrogen atoms is indicated on the right hand scale.

understanding and the modeling of a disordered crystal structure. Our future efforts will be directed to include such information in the structure factor model.

Molecular dynamics simulations allow an estimation of the timescale of the molecular motion and the time spent in low energy and intermediate states. Fig. 5c plots the average root mean square displacement (rmsd) *versus* temperature for non H-atoms, H-atoms attached to C5 and for the other H-atoms. First of all we can see that the H-atoms attached to C5 are more mobile at all temperatures and H-atoms are a bit more mobile than the C N and O atoms due to their smaller mass. Furthermore, we can see that the rmsd for the C5 hydrogen atoms is low below a threshold of 30 K and suddenly increases above this, indicating onset of pronounced rotational movement. However, the rmsd is not indicative of how often the conformations change. A single rotation causes almost the same rmsd increase as multiple ones. Hence we also plotted the number of conformational changes that we counted manually from the torsion angle plots such as shown in Fig. 5b. The temperature dependence of the rotational motion agrees well with the result obtained from X-ray diffraction. We can not observe any rotation below 30 K in the simulations. We assign the observation of some small difference density from X-ray diffraction earlier to zero-point motion. This quantum effect can not be reproduced by molecular mechanics. It is also conceivable that the timescale of the rotation at 10 K is larger than the length of the molecular dynamics simulation. Thus not all rotations that might happen during the time span of the X-ray data collection ($\approx$6 hours) can be modeled in short simulations.

5. Conclusion

The rotational disorder of a single methyl group makes Me-AIB an interesting molecule to study. As X-ray data contain both the effect of thermal motion and the underlying molecular electron density, direct observation of the nature of disorder is usually difficult. Thanks to the flexibility of the parameters of the Hansen & Coppens multipole model in describing electron density and effects of thermal motion simultaneously, disorder in the crystal can be clearly studied. By employing electron density differences on a grid, we visualized rotational disorder of the ester methyl group and relate it to differences seen for the carboxyl group. The comparison of the electron density obtained from a low-parameter multipole model and the electron density predicted by invariom scattering factors—using data measured at five different temperatures—allows us to observe the reduction of rotational disorder at low temperature. Complete freezing of the motion is not observed; the need for improvements in scattering models combining the aspherical electron density and proper treatment of disorder remains even at very low

temperatures. A novel aspect of this study is that molecular dynamics can provide independent information about thermal motion in a crystal structure. Incorporation of this information in the structure factor model will have important implications for refinement of disordered parts of protein structures and for electron-density research of normal resolution structures, objectives which we will pursue in the future.

Acknowledgements

This work was supported by the DFG, grant DI 921/3-1 and the Australian Synchrotron Research Program (ASRP), which is funded by the Commonwealth of Australia under the Major National Research Facilities Program. B.D. thanks the HASYLAB/DESY for category II project access and the STFC and the SRS Daresbury Facility for beam time. Computer time was allocated under the merit allocation scheme of the National Computational Infrastructure (Australia). Help from S. Johnas for the oblique incidence correction for the HASYLAB data and assistance from C. B. Hübschle (Fig. 2) is acknowledged.

References

1 S. Hirokawa and S. Kuribayashi, The crystal structure of alpha-amino isobutyric acid, *Bull. Chem. Soc. Jpn*., 1952, **23**, 192–195.
2 D. E. Lynch and I. McClenaghan, 'Redetermination of α-ammonio-α-methylpropionoate, *Acta Crystallogr., Sect. E*, 2002, **58**, o706–o707.
3 M. Prager and A. Heidemann, Rotational tunneling and neutron spectroscopy: A compilation, *Chem. Rev*., 1997, **97**, 2933–2966.
4 P.-G. Jönsson, Hydrogen bond studies. XLIV. Neutron diffraction study of acetic acid, *Acta Crystallogr., Sect. B*, 1971, **27**, 893–898.
5 M. R. Johnson, M. Neumann, B. Nicolai, P. Smith and G. J. Kearley, The origin and temperature dependence of the single particle, methyl-group rotational potential in acetic acid, *Chem. Phys*., 1997, **215**, 343–353.
6 C. C. Wilson, Zero point motion of the librating methyl group in *p*-hydroxyacetanilide, *Chem. Phys. Lett*., 1997, **280**, 531–534.
7 P. Schiebel, R. J. Papoular, H. Zimmermann, A. Detken, U. Haeberlen and W. Prandl, Isotope induced proton ordering in partially deuterated aspirin, *Phys. Rev. Lett*., 1999, **83**(5), 975–978.
8 C. C. Wilson, Variable temperature study of the crystal structure of paracetamol (p-hydroxyacetanilide) by single crystal neutron diffraction, *Z. Kristallogr*., 2000, **215**, 693–701.
9 C. C. Wilson, The evolution of hydrogen atom parameters under changing external conditions by time-of-flight single crystal neutron diffraction, *Crystallogr. Rev*., 2007, **13**, 143–198.
10 A. Parkin, C. C. Seaton, N. Blagden and C. C. Wilson, Designing hydrogen bonds with temperature-dependent proton disorder. The effect of crystal environment, *Cryst. Growth Des*., 2007, **7**, 531–534.
11 B. Dittrich, T. Koritsánszky and P. Luger, A simple approach to nonspherical electron densities by using invariom, *Angew. Chem., Int. Ed*., 2004, **43**, 2718–2721.
12 B. Dittrich, C. B. Hübschle, P. Luger and M. A. Spackman, Introduction and validation of an invariom database for amino acid, peptide and protein molecules, *Acta Crystallogr., Sect. D*, 2006, **62**, 1325–1335.
13 B. Dittrich, C. B. Hübschle, M. Messerschmidt, R. Kalinowski, D. Girnt and P. Luger, The invariom model and its application: Refinement of DL-serine at different temperatures and resolution, *Acta Crystallogr., Sect. A*, 2005, **61**, 314–320.
14 R. F. Stewart, Electron population analysis with rigid pseudo-atoms, *Acta Crystallogr., Sect. A*, 1976, **32**, 565–574.
15 N. K. Hansen and P. Coppens, Testing aspherical atom refinements on small-molecule data sets, *Acta Crystallogr., Sect. A*, 1978, **34**, 909–921.
16 C. B. Hübschle, P. Luger and B. Dittrich, Automation of invariom and of experimental charge density modelling of organic molecules with the preprocessor program InvariomTool, *J. Appl. Crystallogr*., 2007, **40**, 623–627.
17 P. M. Dominiak, A. Volkov, X. Li, M. Messerschmidt and P. Coppens, A theoretical databank of transferable aspherical atoms and its application to electrostatic interaction energy calculations of macromolecules, *J. Chem. Theory Comput*., 2007, **2**, 232–247.
18 B. Zarychta, V. Pichon-Pesme, B. Guillot, C. Lecomte and C. Jelsch, On the application of an experimental multipolar pseudo-atom library for accurate refinement of small-molecule and protein crystal structures, *Acta Crystallogr., Sect. A*, 2007, **63**, 108–125.
19 M. Karplus and J. A. McCammon, Molecular dynamics simulations of biomolecules, *Nat. Struct. Biol*., 2002, **9**, 646–652.
20 A. Gavezzotti, A molecular dynamics test of the different stability of crystal polymorphs under thermal strain, *J. Am. Chem. Soc*., 2000, **122**, 10724–10724.
21 A. Gavezzotti, Molecular aggregation of acetic acid in a carbon tetrachloride solution: A molecular dynamics study with a view to crystal nucleation, *Chem.–Eur. J*., 1999, **5**, 567–576.
22 W. Kabsch, Automatic processing of rotation diffraction data from crystals of initialy unknow symmetry and cell constants, *J. Appl. Crystallogr*., 1993, **26**, 795–800.
23 G. Wu, B. L. Rodrigues and P. Coppens, The correction of reflection intensities for incomplete absorbtion of high-energy X-ray in the CCD phosphor, *J. Appl. Crystallogr*., 2002, **35**, 356–359.
24 S. K. J. Johnas, W. Morgenroth and E. Weckert, *Oblique incidence correction Hasylab Jahresbericht*, 2006.
25 R. J. Cernik, W. Clegg, R. A. Catlow, G. Bushnell-Wye, J. V. Flaherty, G. Neville Greaves, I. Burrows, D. J. Taylor, S. J. Teat and M. Hamichi, A new high-flux chemical and materials crystallography station at the SRS daresbury. 1. Design, construction and test results, *J. Synchrotron Radiat*., 1997, **4**, 279–286.
26 *SMART and SAINT data collection and processing software for the SMART System*, Bruker AXS Inc., Madison WI, 1995–2007.
27 G. M. Sheldrick, *SADABS version 2007/5 A program for area detector absorption and other corrections*, Technical report University of Göttingen Germany, 2007.
28 G. M. Sheldrick, A short history of SHELX, *Acta Crystallogr., Sect. A*, 2008, **64**, 112–122.
29 T. Koritsánszky, T. Richter, P. Macchi, A. Volkov, C. Gatti, S. Howard, P. R. Mallinson, L. Farrugia, Z. W. Su and N. K. Hansen, *XD–a computer program package for multipole refinement and topological analysis of electron densities from diffraction data*, Technical report Freie Universität Berlin, Berlin, 2003.
30 T. Koritsánszky, A. Volkov and P. Coppens, Aspherical-atom scattering factors from molecular wave functions. 1. Transferability and conformation dependence of atomic electron densities of peptides within the multipole formalism, *Acta Crystallogr., Sect. A*, 2002, **58**, 464–472.
31 A. Ø. Madsen, H. O. Sørensen, C. Flensburg, R. F. Stewart and S. Larsen, Modeling of the nuclear parameters for H atoms in X-ray charge density studies, *Acta Crystallogr., Sect. A*, 2004, **60**, 550–561.
32 P. Munshi, A. Ø. Madsen, M. A. Spackman, S. Larsen and R. Destro, Estimated H-atom anisotropic displacement parameters: A comparison between different methods and with neutron diffraction results, *Acta Crystallogr., Sect. A*, 2008, **64**, 465–475.
33 A. Ø. Madsen, SHADE web server for estimation of hydrogen anisotropic displacement parameters, *J. Appl. Crystallogr*., 2006, **39**, 757–758.
34 V. Schomaker and K. N. Trueblood, On the rigid-body motion of molecules in crystals, *Acta Crystallogr., Sect. B*, 1968, **24**, 63–76.
35 T. Koritsánszky, R. Flaig, D. Zobel, H.-G. Krane, W. Morgenroth and P. Luger, Accurate experimental electronic properties of DL-proline monohydrate obtained within 1 day, *Science*, 1998, **279**, 356–358.

 This journal is © the Owner Societies 2009

36 J. C. Phillips, R. Braun, W. Wang, J. Gumbart, E. Tajkhorshid, E. Villa, C. Chipot, R. D. Skeel, L. Kale and K. Schulten, Scalable molecular dynamics with NAMD, *J. Comput. Chem.*, 2005, **26**, 1781–1802.
37 A. D. MacKerell, Jr., D. Bashford, M. Bellott, R. L. Dunbrack, Jr., J. D. Evanseck, M. J. Field, S. Fischer, J. Gao, H. Guo, S. Ha, D. Joseph-McCarthy, L. Kuchnir, K. Kuczera, F. T. K. Lau, C. Mattos, S. Michnick, T. Ngo, D. T. Nguyen, B. Prodhom, W. E. Reiher, B. Roux, M. Schlenkrich, J. C. Smith, R. Stote, J. Straub, M. Watanabe, J. Wiorkiewicz-Kuczera, D. Yin and M. Karplus, All-atom empirical potential for molecular modeling and dynamics studies of proteins, *J. Phys. Chem. B*, 1998, **102**, 3586–3616.
38 M. J. Frisch, *et al.*, *Gaussian 98 (Revision A.7)*, Technical report Gaussian, Inc., Pittsburgh PA, 1998.
39 T. Darden, D. York and L. Pedersen, Particle mesh Ewald: An $n \log(n)$ method for Ewald sums in large systems, *J. Chem. Phys.*, 1993, **98**, 10089–10092.
40 U. Essmann, L. Perera, M. L. Berkowitz, T. Darden, H. Lee and L. G. Pedersen, A smooth particle mesh Ewald method, *J. Chem. Phys.*, 1995, **103**, 8577–8593.
41 M. N. Burnett and C. K. Johnson, *ORTEP-III, Oak Ridge thermal ellipsoid plot program for crystal structure illustrations*, Technical report Oak Ridge National Laboratory Report ORNL-6895 Oak Ridge, Tennessee, 1996.
42 B. Dittrich, P. Munshi and M. A. Spackman, Re-determination and invariom model refinement of L-ornithine hydrochloride, *Acta Crystallogr., Sect. B*, 2007, **63**, 505–509.
43 P. W. Betteridge, J. R. Carruthers, R. I. Cooper, K. Prout and D. J. Watkin, Crystals version 12: Software for guided crystal structure analysis, *J. Appl. Crystallogr.*, 2003, **36**, 1487.
44 B. Dittrich and M. A. Spackman, Can the interaction density be measured? The example of the non-standard amino acid sarcosine, *Acta Crystallogr., Sect. A*, 2007, **63**, 426–436.
45 F. L. Hirshfeld, Can X-ray data distinguish bonding effects from vibrational smearing?, *Acta Crystallogr., Sect. A*, 1976, **32**, 239–244.
46 F. L. Hirshfeld, Electron density distributions in molecules, *Crystallogr. Rev.*, 1991, **2**, 169–204.
47 E. Keller and J.-S. Pierrard, *SCHAKAL99*, Technical report University of Freiburg, Germany, 1999.
48 W. Humphrey, A. Dalke and K. Schulten, VMD-visual molecular dynamics, *J. Mol. Graphics*, 1996, **14**, 33–38.